



NLR-TP-2000-169

## **Effects of wind tunnel side-plates on airframe noise measurements with phased arrays**

S. Oerlemans and P. Sijtsma



NLR-TP-2000-169

## Effects of wind tunnel side-plates on airframe noise measurements with phased arrays

S. Oerlemans and P. Sijtsma

The contents of this report have been initially prepared for publication as AIAA paper 00-1938 in the proceedings of the 6<sup>th</sup> AIAA/CEAS Aeroacoustics Conference, Lahaina, Hawaii, USA, 6-8 June 2000.

The contents of this report may be cited on condition that full credit is given to NLR and the author(s).

Division: Fluid Dynamics  
Issued: 4 April 2000  
Classification of title: Unclassified



**Contents**

<b>Nomenclature</b>	3
<b>I. Introduction</b>	4
<b>II. Test set-up</b>	5
<b>III. Calibration source</b>	5
<b>IV. Measurements between hard side-plates</b>	6
<b>V. Simulations with infinite side-plates</b>	6
<b>VI. Measurements between lined side-plates</b>	7
<b>VII. Conclusions</b>	8
<b>Acknowledgement</b>	8
<b>References</b>	8

12 Figures

(13 pages in total)



## Nomenclature

### Roman

$a$	mouthpiece radius
$b$	distance between side-plates
$c$	speed of sound
CAA	Computational AeroAcoustics
$f$	frequency
$F_n$	defined in equation (8)
$h$	$z$ -coordinate of monopole source
$H_0^{(2)}$	zero-th order Hankel function of the second kind
$i$	imaginary unit
$k$	wave number ( $=2\pi/\lambda$ )
$M$	Mach number
$p$	sound pressure
$r$	defined in equation (9)
$R$	distance to monopole source
SPL	Sound Pressure Level
$x$	streamwise coordinate
$y$	(horizontal) coordinate perpendicular to array plane
$z$	vertical coordinate
$Z$	wall impedance

### Greek

$\delta$	end correction
$\Delta$	distance between reference microphone and open end of mouthpiece
$\varepsilon_n$	solutions of equation (7)
$\lambda$	wavelength
$\rho$	air density
$\xi$	$x$ -coordinate of monopole source
$\eta$	$y$ -coordinate of monopole source
$\zeta$	$z$ -coordinate of monopole source

### Indices

refmic	reference microphone in mouthpiece
dev	deviation from theoretical monopole
array	calculated by array software

## EFFECTS OF WIND TUNNEL SIDE-PLATES ON AIRFRAME NOISE MEASUREMENTS WITH PHASED ARRAYS

Stefan Oerlemans\* and Pieter Sijtsma†

*National Aerospace Laboratory NLR, 8300 AD Emmeloord, The Netherlands*

A convenient method for airframe noise measurements in an open jet acoustic wind tunnel is the combination of an out-of-flow phased array with a semi-open test section consisting of two side-plates between which a model can be mounted. In this paper the effects of these side-plates on acoustic measurements with a phased array are investigated both experimentally and theoretically. First, a set-up with hard wooden side-plates and a cross-shaped array was tested. Calibration measurements with a monopole source placed between the plates showed errors in source strength up to 10 dB, with strong dependence on frequency and source location. A theoretical study identified acoustic interference (standing waves) between the hard plates as the cause of this inaccuracy. Theory predicted much better results when the cross-shaped array was replaced by a sparse array and the hard plates by acoustically lined plates. After application of these modifications in the test set-up, new calibration measurements indeed showed impressive improvement in the ability to determine absolute levels with a phased array. True monopole source levels were recovered within 2 dB for frequencies up to 8 kHz and a tunnel flow speed up to  $M = 0.22$ . Moreover, the measured source level was practically independent on the source location.

### I. Introduction

To understand the source mechanisms of airframe noise components, such as leading edge noise, trailing edge noise, slat noise and flap side edge noise, and to be able to validate (CAA) predictions, detailed measurements on generic models are required. To avoid interaction of the model with the open jet shear layer turbulence, a convenient set-up for such measurements is to extend opposite edges of the nozzle of an open jet acoustic wind tunnel with hard side-plates. The model is placed between these plates and acoustic measurements are carried out with a phased array out of the flow. This paper is focussed on the effects of these side-plates. The concept is applied by NLR (Ref. 1), NASA (Ref. 2), and other institutes.

A set-up with these hard side-plates should, however, not be applied without being very careful with the interpretation of the results. In

general the phased array software locates the noise sources on the correct spots, but the recovered levels may be completely wrong. There are several reasons for that.

First of all, the array software assumes compact monopole sources with a uniform directivity. In reality, the sources are dipoles, quadrupoles or other multi-poles which may be distributed along edges, having a certain correlation length. Secondly, the array software assumes 100% coherence under different emission angles, but for airframe noise sources this needs not be the case. Moreover, when the sound propagates through the shear layer, the turbulence herein can cause extra loss of angular coherence. Because of these effects, the recovered source levels may depend on the size of the array and on the applied beamforming algorithm (Ref. 2). This uncertainty can be overcome by scaling the recovered source levels using the total level measured by the microphone array.

Another very important source of error is the presence of hard side-plates. Reflections between these plates cause interference patterns, which can extend to the microphone array. Although an acoustic array may be able to physically separate the source from its mirror sources, the reflections can lead to large differences between the levels recovered by the array software and the true levels. Moreover, the errors between recovered

---

\* Research Engineer, Aeroacoustics Department, P.O. Box 153, Email: stefan@nlr.nl.

† Research Engineer, Aeroacoustics Department, P.O. Box 153, Email: sijtsma@nlr.nl.

Copyright © 2000 by the National Aerospace Laboratory NLR. Published by the American Institute of Aeronautics and Astronautics, Inc. with permission.



levels and true levels will depend strongly on the position of the source and on the frequency. Measurements in a reverberant environment can lead to errors up to 10 dB. In Ref. 3, the same phenomenon was found for a closed wind tunnel test section.

In this paper the effects of wind tunnel side-plates on acoustic measurements with phased arrays will be investigated both experimentally and theoretically. It will be demonstrated that a drastic improvement in the ability to recover source strengths is obtained by replacing hard side-plates by lined plates and a cross array by a sparse array.

The starting point will be a description of the NLR wind tunnel set-up for airframe noise measurements (Section II). For calibration measurements, a special monopole source was used, which is described in Section III.

Section IV reviews the results of first calibration measurements, in which the monopole source was placed at a number of positions between the hard side-plates and acoustic measurements were carried out with a cross-shaped array of 23 microphones.

Section V describes simulations for hard side-plates in combination with the cross array, and for lined side-plates with a sparse array.

In Section VI experimental results will be presented of calibration measurements for a modified test set-up with lined side-plates and a sparse array design.

The conclusions are given in Section VII.

## II. Test set-up

The experiments were performed in NLR's Small Anechoic Wind Tunnel KAT. A photographic and a schematic picture of the set-up are given in Fig. 1a and Fig. 1b, respectively. The KAT is an open circuit wind tunnel, surrounded by a  $5.5 \times 5 \times 3$  m<sup>3</sup> room which is completely covered with 0.3 m foam wedges, yielding more than 99% absorption above 500 Hz. Two horizontal side-plates are mounted to the upper and lower sides of the rectangular  $0.38 \times 0.51$  m<sup>2</sup> nozzle, providing a semi-open test section for airfoil self-noise measurements. The maximum wind speed is 75 m/s.

In a first series of experiments, hard wooden side-plates were used in combination with a cross-

shaped array of 23 microphones (Fig. 2).

In the second series, the hard side-plates were replaced by 5% open perforated plates backed with a 5.5 cm layer of acoustic foam. Further, a sparse array design of 35 microphones was implemented (Fig. 2). Calibration measurements were performed with a monopole source (to be described in Section III) in an anechoic environment and between the side-plates, with and without flow.

## III. Calibration source

The calibration source is an acoustic monopole source, owned by the Institute of Applied Physics TNO-TPD (Ref. 4). This source features a flexible tube, which is on one end excited with broadband noise by an acoustic driver. The other end of the tube is connected to a mouthpiece having a circular opening with radius  $a = 3.5$  mm. The acoustic pressure at the open end is measured with a pressure transducer inside the mouthpiece at a distance  $\Delta = 10$  mm from the opening.

If the frequency is sufficiently low, say  $ka < 0.3$ , where  $k = 2\pi f/c$ ,  $f$  is the frequency and  $c$  is the sound speed, then from this open end an omnidirectional sound field is radiating, i.e., an acoustic monopole. For higher frequencies directivity effects increase, but in the direction of the array the angular differences are small ( $< 2$  dB) for frequencies up to  $ka \approx 0.5$ .

The coherence of the monopole source was determined from the signals on different array microphones, and was found to be almost 100% for frequencies up to 8 kHz in an anechoic environment. This high coherence level is confirmed by Fig. 3, where the array output (using conventional beamforming) can be seen to be practically identical to the true source level obtained from the average sound pressure level at the array microphones.

The level of the monopole source is directly related to the level at the reference transducer. If  $ka \ll 1$ , the following relation can be derived between the sound pressure in the tube and the sound pressure at a distance  $R$  from the source (i.e., the open end of the tube):

$$\left| \frac{p(R)}{p_{\text{refmic}}} \right| = \frac{a^2 k}{4R \sin(k(\Delta + a\delta))}, \quad (1)$$

where  $\delta \approx 0.6$  is the end correction.

An interesting quantity to look at is:

$$\text{SPL}_{\text{dev}} = \text{SPL}_{\text{array}} - \text{SPL}_{\text{refmic}} + 20 \log \left( \frac{a^2 k}{4 \sin(k(\Delta + a\delta))} \right), \quad (2)$$

where  $\text{SPL}_{\text{array}}$  is the sound pressure level at 1 m, as calculated by the array software, and  $\text{SPL}_{\text{refmic}}$  is the sound pressure level measured by the reference transducer. The quantity  $\text{SPL}_{\text{dev}}$  represents the deviation of the experimental monopole source from the theoretical monopole described by equation (1). Thus, theoretically  $\text{SPL}_{\text{dev}}$  should be identically zero, at least as long the assumption  $ka \ll 1$  holds.

#### **IV. Measurements between hard side-plates**

In order to calibrate the test set-up, the monopole source was placed at a number of positions between the hard side-plates and acoustic measurements were carried out with the cross array. Large microphone-to-microphone differences indicated a strong interference pattern. Fig. 4 shows the recovered source levels at the maximum in the acoustic source plot as a function of the position of the monopole source between the hard side-plates. These source levels were obtained by conventional beamforming.

As a reference the true source level, determined with the sparse array in an anechoic environment, is also given. The figure shows errors in source level of more than 10 dB with strong dependence on source position and frequency.

#### **V. Simulations with infinite side-plates**

In order to study theoretically the effect of array layout and plate lining, simulations were carried out in which the side-plates were assumed to be infinite. The plates were located in the planes  $z = \pm \frac{1}{2}b$ . For convenience, only the upper plate was modelled as acoustically soft. Lining on both plates was in principle possible, but would have required a complicated eigenvalue search routine. The simulations were carried out without flow.

The acoustic pressure field of a monopole source in  $(\xi, \eta, \zeta)$  can be obtained by solving the equation:

$$\nabla^2 p + k^2 p = \delta(x - \xi)\delta(y - \eta)\delta(z - \zeta), \quad (3)$$

with hard wall boundary condition at the lower plate:

$$\frac{\partial p}{\partial z}(x, y, -\frac{1}{2}b) = 0 \quad (4)$$

and an impedance wall condition at the upper plate:

$$\frac{-ikp(x, y, \frac{1}{2}b)}{\frac{\partial p}{\partial z}(x, y, \frac{1}{2}b)} = \frac{Z}{\rho c}, \quad (5)$$

where  $Z$  is the wall impedance and  $\rho$  is the air density. The solution is:

$$p = \frac{i}{2} \sum_{n=0}^{\infty} F_n(z, \zeta) H_0^{(2)}\left(r\sqrt{k^2 - \varepsilon_n^2}\right), \quad (6)$$

in which  $H_0^{(2)}$  is the zero-th order Hankel function of the second kind,  $\varepsilon_n$  are the solutions of

$$\frac{ik \cos(\varepsilon_n b)}{\varepsilon_n \sin(\varepsilon_n b)} = \frac{Z}{\rho c} \quad (7)$$

and further:

$$F_n(z, \zeta) = \frac{\cos(\varepsilon_n(z + \frac{1}{2}b))\cos(\varepsilon_n(\zeta + \frac{1}{2}b))}{b + \frac{\sin(2\varepsilon_n b)}{2\varepsilon_n}}, \quad (8)$$

$$r = \sqrt{(x - \xi)^2 + (y - \eta)^2}. \quad (9)$$

Now suppose that the distance between the side-plates is  $b = 0.5$  and a monopole is located in  $(-0.25, 0, 0)$ , having a strength such that the SPL at 1 m from the source would be 60 dB in an anechoic environment.

We will first simulate the hard wall/cross array situation, for comparison with the preceding section. This means that the impedance of the upper plate is infinite:  $Z = \infty$ . Then in the plane  $y = -0.05$ , which is close to the source, the acoustic field is as drawn in Fig. 5. This example is calculated for frequency  $f = 2400$  Hz. The monopole is clearly visible, but interference patterns can also be seen.

In Fig. 6, the acoustic field is shown in the plane  $y = -0.6$ , which is the plane of the array. Also a part of the cross array is drawn. In this plot, a monopole can not be recognised anymore. In

other words, at a distance of 60 cm from the source, only interference patterns are left from the original monopole field.

In the same way as described above, microphone signals of the cross array can be simulated. With these simulated signals (again at  $f = 2400$  Hz), we can try to recover the source strength by scanning the plane  $y = 0$  with a conventional beamforming algorithm, using the free space Green's function to define the "steering vectors". The result is shown in Fig. 7, where the levels have been scaled to SPL at 1 m distance.

In Fig. 7, the source location  $(-0.25, 0, 0)$  has been recovered convincingly. This is an amazing result, knowing the large distortion of the sound field in the plane of the array (Fig. 6). The stretching of the main lobe and the appearance of the side lobe are just artefacts of the cross-shape of the array.

There is, however, one thing to notice, namely the predicted level. This is more than 65 dB, while it should be 60 dB: a remarkable error for a source which was found so well. To explain this, we have to look again at Fig. 6. Many microphones in the horizontal arm of the array happen to be situated in a node of the interference pattern. This explains why the recovered level is too high.

For other frequencies and/or other source locations, the interference pattern at  $y = -0.6$  is different and, hence, other source levels will be found. This is demonstrated in Fig. 8, where the errors in the source level are plotted against frequency for different source locations between the hard side-plates. A spreading of more than 10 dB is found, which is the same order of magnitude as with the hard wall measurements described in the preceding section (cf. Fig. 4).

To reduce this unwanted inaccuracy, two modifications were made. First, the cross array was replaced by the sparse array shown in Fig. 2. The design of this array is based on the same principle as in Ref. 3. Herewith, the risk of having many microphones simultaneously in a node or in an antinode is reduced, so that the array is less sensitive to interference patterns. Secondly, plate lining was applied to suppress the development of standing waves.

To demonstrate the merits of these modifications, simulations were made with a frequency-independent plate impedance  $Z = (3 - i)\rho c$ . Source error plots similar to those in Fig. 8 are plotted in Fig. 9. It is clear that a drastic reduction of the source level errors is achieved. The largest deviation is seen for  $h = 0.20$ , at low frequencies. This is because  $h = 0.20$  is the closest to the (lined) wall and, at lower frequencies, the lobes of the main source and the mirror source are interfering.

In reality, even better performance may be expected, since in the simulations described above only one side-plate is lined. Furthermore, for convenience a locally reacting lining model was used, which still produces mirror sources, though with a reduced level. The best performance is expected for wall treatment with maximum absorption (e.g. as in Ref. 5).

#### **VI. Measurements between lined side-plates**

To check the predicted improvements, plate lining and sparse array design were also applied to the experimental set-up. For the lining, a 5% open perforated plate, backed with 5.5 cm acoustic foam was applied. Although this perforated plate limits the acoustic effectiveness, it preserves the flow quality in the test section. A better, but also much more expensive, way of lining is described in Ref. 5.

The set-up with lined side-plates was calibrated using the sparse array and the monopole source described in section III. In Fig. 10 recovered levels are given for the monopole source in an anechoic environment and between the lined side-plates. For comparison the recovered level with the source at the same position between the *hard* side-plates (cf. Fig. 4) is also given. This figure shows the drastic improvement that is obtained by lining the side-plates. Whereas hard side-plates caused frequency dependent errors up to almost 10 dB, with lined side-plates the correct level is recovered within 2 dB for frequencies higher than 1 kHz. Even better results may be obtained when the acoustic absorption of the lining is further increased. However, this has to be done carefully, i.e., without spoiling the 2D flow characteristics.

The influence of source position between the lined side-plates on the recovered levels was investigated with a monopole source similar to the one described in section III ( $a = 3.5$  mm,  $\Delta = 10$  mm). Fig. 11 shows the recovered source levels for a number of source positions. It can be





seen that, in contrast to the hard side-plate measurements, the position of the source has no large influence on the recovered source level, even when the source is located close to the side-plates ( $z = -0.18$ ).

It is also interesting to look at the influence of tunnel flow. Therefore, let us consider two measurements with the monopole source of section III, one without flow, the other with tunnel Mach number  $M = 0.22$ . The source was built into a streamline profile to suppress aerodynamic noise. In both cases, the source is located at  $(0,0,0)$ . In case of flow, the monopole source is located inside the jet flow, while the array is outside. Therefore, to recover the source strength by conventional beamforming, a correction has to be made for the shear layer.

This correction is as follows. For the definition of the "steering vectors", the free space Green's function in the presence of uniform flow (Ref. 6) was used. However, in this Green's function, the *average* flow speed between source and microphone is inserted. This modelling is not as sophisticated as the Amiet correction (Ref. 7), but a comparison did not reveal noticeable differences. Even a comparison with a ray acoustics model (Ref. 8), incorporating the finite thickness of the shear layer, did not lead to significant differences.

The influence of flow on the recovered source level is shown in Fig. 12. This figure shows that the differences remain within a few dB up to 8 kHz, except at low frequencies, where the tunnel noise is dominant.

## **VII. Conclusions**

The effects of wind tunnel side-plates on acoustic measurements with phased arrays were investigated both experimentally and theoretically. Calibration measurements with a monopole source showed that in case of hard side-plates in combination with a cross array, source level errors up to 10 dB occur which strongly depend on frequency and source position. In a theoretical study these inaccuracies could be attributed to standing waves between the side-plates. The theory predicted much better performance for lined side-plates and a sparse array design. This was confirmed in calibration measurements with a modified test set-up: source strengths could be determined within 2 dB for

frequencies up to 8 kHz and flow speeds up to  $M = 0.22$ . Moreover, the source levels were practically independent on the source location.

## **Acknowledgement**

The authors are grateful to TNO-TPD for the use of their monopole source. This work has been carried out in the framework of the JOULE project 'Design and Testing of Acoustically Optimized Airfoils for Wind Turbines' (DATA) under contracts awarded by the European Commission and the Netherlands Agency for Energy and Environment, NOVEM BV.

## **References**

1. Dassen, A.G.M, Parchen, R., Bruggeman, J.C., and Hagg, F., Results of a Wind Tunnel Study on the Reduction of Airfoil Self-Noise by the Application of Serrated Blade Trailing Edges, presented at the European Wind Energy Conference and Exhibition, Gothenburg, Sweden, 20-24 May 1996.
2. Brooks, T.F., and Humphreys, W.M. Jr., Effect of Directional Array Size on the Measurement of Airframe Noise Components, AIAA Paper 99-1958, 1999.
3. Sijtsma, P., and Holthusen, H., Source Location by Phased Array Measurements in Closed Wind Tunnel Sections, AIAA Paper 99-1814, 1999 (NLR-TP-99108).
4. Verheij, J.W., Tol, F.W. van, Hopmans, L.H.M., Monopole Airborne Sound Source with in situ measurements of its Volume Velocity, Internoise 1995, Newport Beach, USA, 10-12 July 1995.
5. Soderman, P.T., Schmitz, F.H., Allen, C.S., Jaeger, S.M., Sacco, J.N., Hayes, J.A., Design of a Deep Acoustic Lining for the 40- by 80 Foot Wind Tunnel Test Section, AIAA Paper 99-1938, 1999.
6. Mosher, M., The Influence of a Wind Tunnel on Helicopter Rotational Noise: Formulation of Analysis, NASA Technical Memorandum 85982, 1984.
7. Amiet, R.K., Correction of Open Jet Wind Tunnel Measurements for Shear Layer Diffraction, AIAA Paper 75-532, 1975.
8. Schulten, J.B.H.M., Computation of Aircraft Noise Propagation through the Atmospheric Boundary Layer, Proc. 5<sup>th</sup> Int. Congress on Sound and Vibration, Adelaide, Australia, 1997 (NLR-TP-97374).

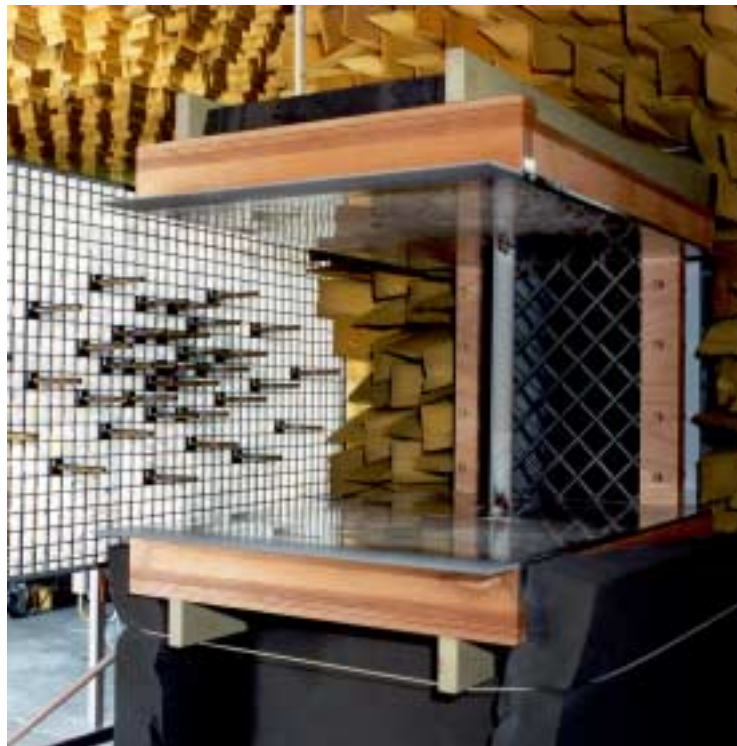


Fig. 1a: KAT set-up for airframe noise measurements, with lined side-plates and a turbulence grid mounted in the nozzle. The 35 microphone sparse array is located on the left.

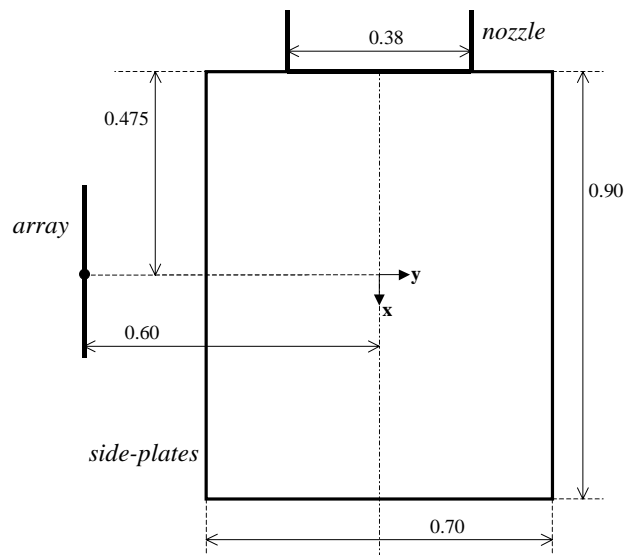


Fig 1b: Top view of set-up for calibration measurements in the Small Anechoic Wind Tunnel (KAT). The flow is in the positive  $x$ -direction. The (hard or lined) side-plates are located at  $z = \pm 0.255$  m. The array centre is placed at the height of the tunnel centre line. Dimensions are in meters.

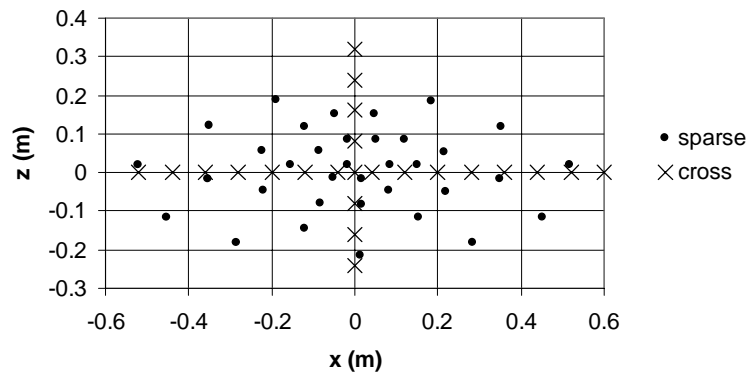


Fig. 2: Cross and sparse array design.

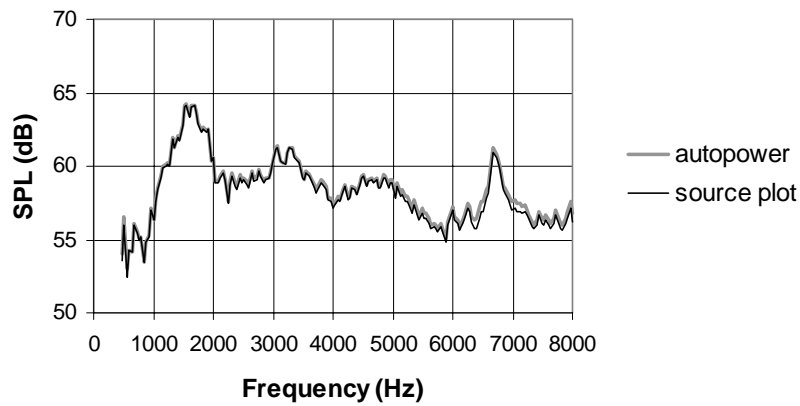


Fig. 3: Comparison of the maximum in the acoustic source plot (conventional beamforming) with the average sound pressure level at the (sparse) array microphones ('autopower'). The experiment was carried out with the monopole source in an anechoic environment.

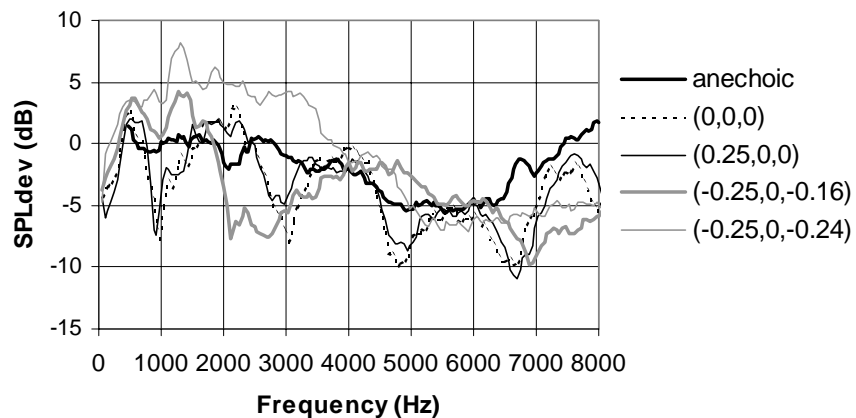


Fig. 4: Comparison of recovered source levels for different monopole source positions  $(x,y,z)$  between the hard side-plates. The source levels were determined with the cross array, from the maximum in the acoustic source plot. As a reference the true, anechoic level is also given.

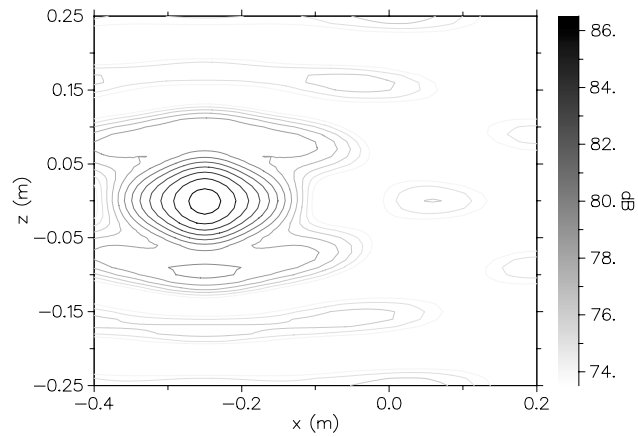


Fig. 5: Simulated pressure field at  $y = -0.05$  of an acoustic monopole at  $(-0.25, 0, 0)$  between infinite, hard side-plates,  $f = 2400$  Hz.

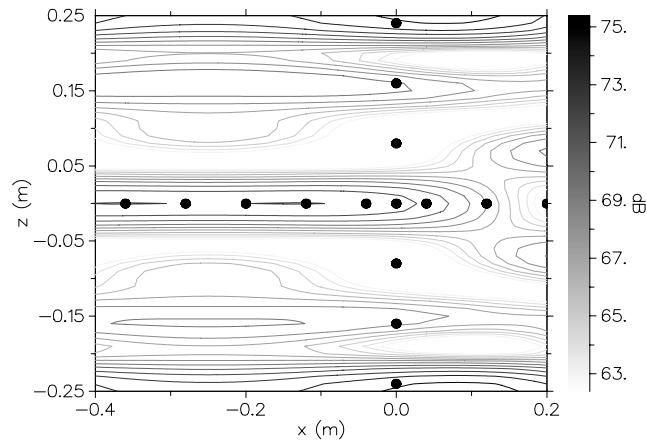


Fig. 6: Simulated pressure field at  $y = -0.6$  of an acoustic monopole at  $(-0.25, 0, 0)$  between infinite, hard side-plates,  $f = 2400$  Hz (with part of the cross array).

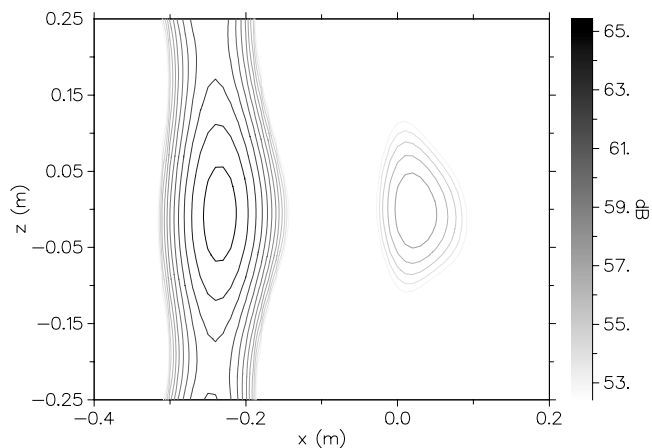


Fig. 7: Simulated acoustic scan in  $y = 0$  with infinite, hard side-plates and cross array,  $f = 2400$  Hz.

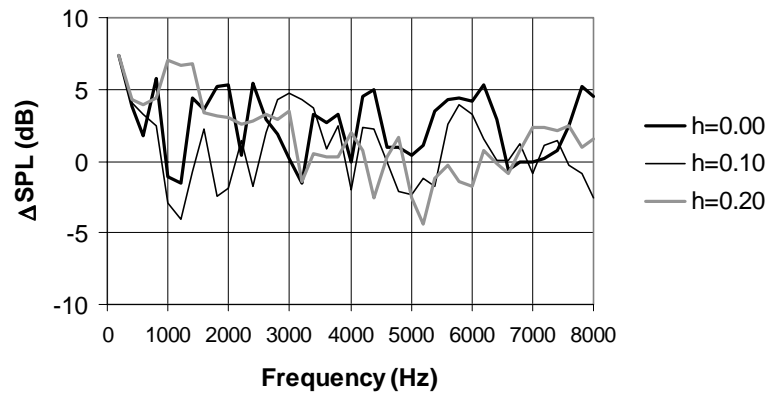


Fig. 8: Simulated source level errors with hard side-plates and cross array, for several source locations  $(-0.25,0,h)$ . The side-plates are located at  $z = \pm 0.25$  m.

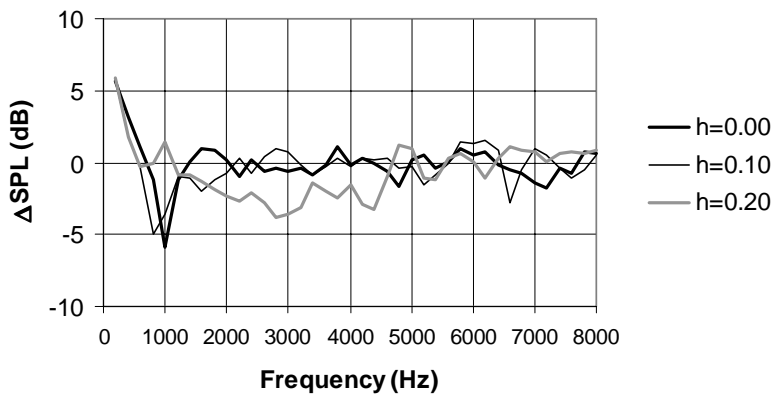


Fig. 9: Simulated source level errors with lined side-plate and sparse array, for several source locations  $(-0.25,0,h)$ . The side-plates are located at  $z = \pm 0.25$  m.

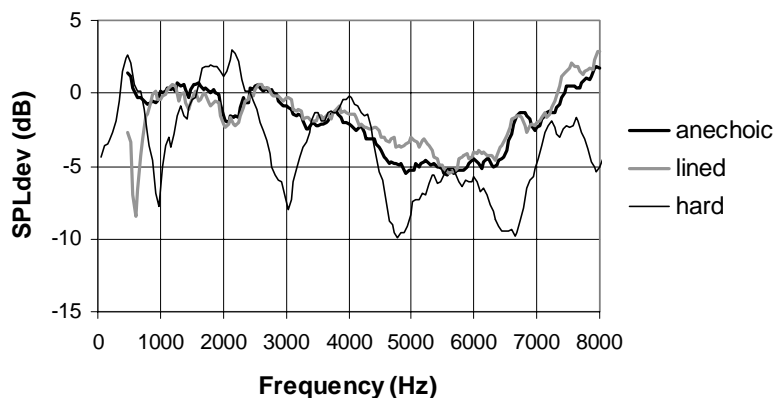


Fig. 10: Comparison of recovered source levels for the monopole source, in an anechoic environment and between the lined and hard side-plates. The source levels were determined with the sparse array (lined side-plates) and cross array (hard side-plates), from the maximum in the acoustic source plot. The source is located at  $(0,0,0)$ , the side-plates at  $z = \pm 0.255$  m.

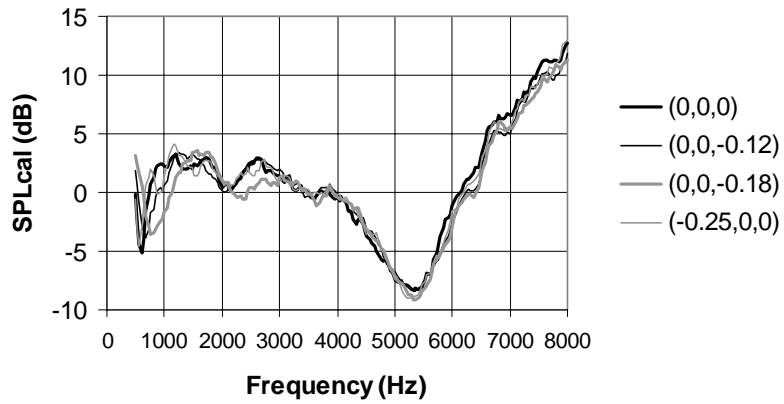


Fig. 11: Comparison of recovered source levels for different monopole source positions  $(x,y,z)$  between the lined side-plates. The source levels were determined with the sparse array, from the maximum in the acoustic source plot.

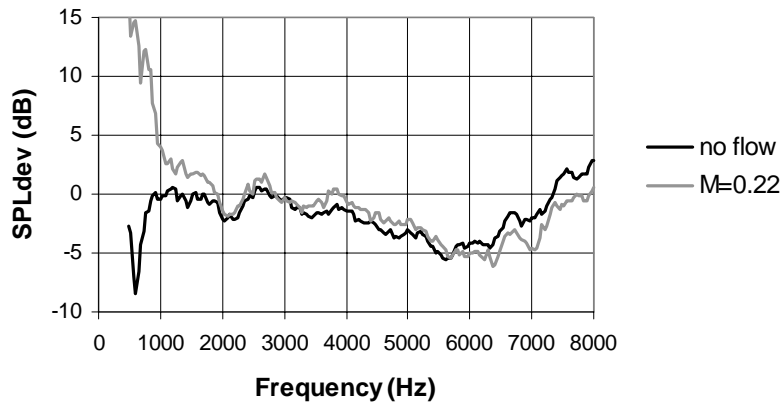


Fig. 12: Recovered source levels with and without tunnel flow, between lined side-plates. The monopole source is located at  $(0,0,0)$ .